Evaluation of multiple-channel OFDM based airborne ultrasonic communications

Wentao Jiang*, William M. D. Wright*

School of Engineering - Electrical and Electronic Engineering, University College Cork, Cork, Ireland

Abstract

Orthogonal frequency division multiplexing (OFDM) modulation has been extensively used in both wired and wireless communication systems. The use of OFDM technology allows very high spectral efficiency data transmission without using complex equalizers to correct the effect of a frequency-selective channel. This work investigated OFDM methods in an airborne ultrasonic communication system, using commercially available capacitive ultrasonic transducers operating at 50 kHz to transmit information through the air. Conventional modulation schemes such as binary phase shift keying (BPSK) and quadrature amplitude modulation (QAM) were used to modulate sub-carrier signals, and the performances were evaluated in an indoor laboratory environment. Line-of-sight (LOS) transmission range up to 11 m with no measurable errors was achieved using BPSK at a data rate of 45 kb/s and a spectral efficiency of 1 b/s/Hz. By implementing a higher order modulation scheme (16-QAM), the system data transfer rate was increased to 180 kb/s with a spectral efficiency of 4 b/s/Hz at attainable transmission distances up to 6 m. Diffraction effects were incorporated into a model of the ultrasonic channel that also accounted for beam spread and attenuation in air. The simulations were a good match to the measured signals and non-LOS signals could be demodulated successfully. The effects of multipath interference were also studied in this work. By adding cyclic prefix (CP) to the OFDM symbols, the bit error rate (BER) performance was significantly improved in a multipath environment.

Keywords:
Airborne ultrasonic communication, binary phase shift keying (BPSK) and quadrature amplitude modulation (QAM) modulation, capacitive ultrasonic transducer, multipath interference, orthogonal frequency division multiplexing (OFDM)

1. Introduction

The use of modulated ultrasound as a way of communication has existed for many years. Most ultrasonic communication systems have been developed for underwater applications because the physical properties of liquids tend to allow sound waves travelling via molecular vibrations to cover relatively long distances. However, there is limited information published in the area of ultrasonic communications in air. This is because sound propagation in air is more difficult, in that it is much more susceptible to changes in atmospheric conditions and attenuation is significant. As ultrasonic signals do not travel long distances in air, it is not surprising that most ultrasonic communication systems are designed for indoor use [1, 2, 3, 4]. One particular aspect of interest is the high security features that are inherent as ultrasound is virtually impossible to detect from outside the room,

*Corresponding author
Email addresses: `w.jiang@umail.ucc.ie` (Wentao Jiang), `bill.wright@ucc.ie` (William M. D. Wright)

eliminating the risks of wireless interception such as Bluesniping and jamming attacks [5, 6]. In addition, in areas with electronics sensitive to electromagnetic interference, ultrasonic transmission is a desirable alternative compared to the use of radio frequency methods.

The attenuation of ultrasound in air at high frequencies is high, which limits the potential transmission bandwidth and range of the communication system. Therefore, to achieve reasonable data rates and practical transmission ranges, it is necessary to apply a suitable communication technique which can make full use of the limited available bandwidth of ultrasonic transducers that operate in air. Orthogonal frequency division multiplexing (OFDM) is a highly efficient form of multicarrier modulation which is extensively used in modern telecommunications, ranging from asymmetric digital subscriber line (ADSL) modem technology to 802.11 Wi-Fi wireless systems [7]. By spreading the data across orthogonal frequency bands, OFDM is also an effective solution to inter-symbol interference (ISI) caused by a dispersive channel. Quadrature amplitude modulation (QAM) is most often used in OFDM to further improve the bandwidth efficiency and data transfer rate. In this paper, both binary phase shift keying (BPSK) and higher order modulation schemes (4-QAM and 16-QAM) are evaluated for ultrasonic communications in air. Problems that occur in OFDM transmissions are also investigated and solutions are given. Section II provides a review of the relevant academic literature in the area of airborne ultrasonic communications and the state of the art of this work in the field. A typical OFDM system for wireless applications is presented in Section III. This is followed by the apparatus and experimental results in Section IV and Section V, respectively. Section VI gives the conclusions of the work.

2. Related work

The first generation batteryless, wireless remote control system for TV receivers was designed by Robert Adler for Zenith televisions in the 1950s [1]. Distinctive high frequency sounds at ultrasonic frequencies of around 40 kHz were produced by striking different lengths of aluminium rod with a set of hammer buttons. These sounds were decoded at the TV, which changed channels appropriately. In [2], an indoor positioning system was developed by emitting frequency shift keying (FSK) modulated ultrasonic signals. In this work, the attainable transmission range achieved was up to 20 m, with a data rate of 100 b/s on a 4 kHz bandwidth at 40 kHz. Another indoor positioning system achieved a ranging accuracy of 2 cm using piezo film ultrasonic transducers [3]. BPSK modulated direct sequence code division multiple access (CDMA) signal structure was used in this work, and achieved a data rate of 20 kb/s on a 76 kHz bandwidth at 50 kHz. Later work on multichannel data communication investigated high frequency amplitude shift keying (ASK) and on-off keying (OOK) at 250 kHz with a 0.5 m transmission distance and achieved an 80 kb/s data transfer rate using prototype transducers [8]. In [4], the authors studied the performance of air-coupled ultrasonic transmission over directional short-range links using OOK, binary frequency shift keying (BFSK) and BPSK modulations. The system started to experience error decoding at a range of 1.6 m and the maximum data rate achieved was 83 kb/s using a physical hard-wired synchronization link between the transmitter and the receiver in a laboratory environment. Another later study by the same authors implemented single-channel quadrature phase shift keying (QPSK) modulation using the same custom-made capacitive transducers in [4] and achieved a bit rate of 200 kb/s over 1.2 m in air in a line-of-sight (LOS) manner [5]. Recent work looked at a 2-channel OFDM scheme for use in localization systems [9]. However, as piezoelectric transducers were used, the achieved data rate was only 5.7 kb/s and the measured packet error rate was 13% at a distance of 18 m.

In this work, multiple-channel OFDM with different order baseband modulation schemes is investigated to achieve the longest error-free decoding range and highest data rate possible using a pair of commercially available capacitive ultrasonic transducers at 50 kHz. The essential problems due to phase noise and multipath interference that OFDM may encounter in practical use are analysed and appropriate solutions are given. Of particular interest are the effects of multipath interference and diffracted non-LOS performance.

3. OFDM system description

3.1. OFDM modulation and demodulation

To enable the largest amount of data to be communicated using a finite frequency range, conventional frequency division multiplexing (FDM) modulation uses relatively small symbol durations. The system then becomes more susceptible to loss of information from impulse noise, multipath distortion and other impairments. FDM also allows each channel to be band-limited to a specific frequency range by implementing a pulse-shaping filter [10]. However, this technique introduces unnecessary waste of the frequency spectrum in guard spaces between the sub-channels. It also increases the complexity of each sub-carrier modulator. OFDM modulation decreases the rate of the original data stream in all parallel sub-carrier channels in order to mitigate multipath interference. By generating overlapping but non-interfering sub-channels, it also maximises the spectral efficiency. In a typical OFDM system sending complex data $\{d_n\}$, N harmonic sinusoids that are orthogonal on a period T_s of the fundamental sub-carrier signal are modulated and combined in parallel, giving the complex envelope $s(t)$ of the OFDM signal:

$$s(t) = \sum_{n=0}^{N-1} d_n e^{j2\pi f_n t} \Pi(t), \tag{1}$$

$$\Pi(t) = \begin{cases} 1, & 0 < t \leq T_s \\ 0, & otherwise. \end{cases} \tag{2}$$

Here, $f_n = n/T_s$, and $\Pi(t)$ represents a rectangular pulse with a duration of T_s. The rectangular window has a sinc-shape spectrum which makes a sub-channel spectrum heavily overlap its neighbours. Take N samples of the pulse $s(t)$ within T_s, the OFDM signal can then be obtained efficiently by an inverse fast Fourier transform (IFFT) [11] of the data sequence $\{d_n\}$:

$$\begin{aligned} s(m) &= \sum_{n=0}^{N-1} d_n e^{j\frac{2\pi}{N}nm} \qquad for\ m \in [0, N-1] \\ &= N \times IFFT\{d_n\}. \end{aligned} \tag{3}$$

At the receiver, the demodulation for an OFDM signal is essentially the reverse process of the modulation. The fast Fourier transform (FFT) is therefore performed on the sampled OFDM signal to recover the data sequence $\{d_n\}$, avoiding the need for complex sub-channel filters.

3.2. Synchronization

Synchronization is a fundamental requirement for any wireless communication system to work properly. Once a data packet is detected, the receiver performs a synchronization operation that identifies the starting point of the packet. Therefore, a preamble is needed at the start of the data packet for wireless synchronization. A linear frequency modulation (LFM) signal whose frequency sweeps linearly from low to high within a certain time is used in this work. It is also the most commonly used signal in practical radar systems for range detection [12]. By performing correlation of a known LFM signal and the received signal using a matched-filter at the receiver, the maximum energy of the matched-filter output then indicates the start of the arriving data sequence. The main advantage of using a LFM signal is that it provides precise timing resolution for frame synchronisation as the matched filter maximises the signal-to-noise ratio (SNR) of the signal [10, 13].

3.3. Phase noise

One of the non-ideal effects that can occur in a real OFDM system is symbol timing offset (STO) which results in a rotated phase in the received constellation [14]. A known LFM preamble is located at the beginning of the data sequence to detect the boundary of the OFDM symbol after matched filtering. However, inaccuracy may still remain, and this leads to an offset in the FFT window location. Assuming the STO is δ samples, the received signal will then be a shifted version of $s(m)$ in (3). After applying the FFT, the recovered complex number sequence y_n for each OFDM symbol can be derived as:

$$\begin{aligned} y_n &= \sum_{m=0}^{N-1} \{s(m+\delta)\} \cdot e^{-j\frac{2\pi}{N}mn} \\ &= \sum_{m=0}^{N-1} \left\{ \sum_{n=0}^{N-1} d_n e^{j\frac{2\pi}{N}n(m+\delta)} \right\} \cdot e^{-j\frac{2\pi}{N}mn} \\ &= d_n \cdot e^{j\frac{2\pi}{N}n\delta}, \qquad n \in [0, N-1]. \end{aligned} \tag{4}$$

As (4) shows, an STO of δ samples in the time domain incurs a phase offset of $\frac{2\pi}{N}n\delta$ in the frequency domain, which is proportional to the sub-carrier index n, as well as the STO. This means that the symbol timing error does not destroy the orthogonality of the sub-carriers, and the effect of the timing error is a phase rotation which changes linearly with the carrier index.

STO can be corrected by applying the maximum likelihood (ML) approach [10] to the data-aided phase recovery scheme. Mathematically, the maximisation can be expressed as:

$$\hat{\delta} = \arg\max_{\delta} \left\{ \sum_{m=0}^{N-1} s(m)s(m+\delta) \right\}. \tag{5}$$

The sum in equation (5) is actually the time-correlation between the received signal $s(m+\delta)$ and the signal of interest $s(m)$. Therefore, in this particular case, the ML approach is equivalent to the maximisation of the correlation.

3.4. OFDM in a multipath environment

The main advantage of OFDM over other forms of modulation is that it is much easier to make it immune to ISI caused by multipath propagation. In a linear dispersive channel, the received signal sequence, $r(m)$, can be expressed as the sum of several versions of the transmitted signal with different gains and delays:

$$r(m) = \sum_{i=0}^{L-1} \alpha_i s(m-\delta_i), \tag{6}$$

where L is the number of multipath components, α_i are path attenuation factors and δ_i are path delays. ISI could be easily eliminated by adding guard intervals (GI) between different OFDM symbols. As long as the length of the GI is larger than the maximum estimated delay spread, the effect of ISI can then be completely removed. However, if the GI is left empty, it will lead to another type of interference called inter-carrier interference (ICI) as the zero-padded waveform would destroy the orthogonality between sub-carriers. Therefore, to prevent both ISI and ICI, an OFDM symbol is usually cyclically extended into the GI. This is achieved by taking the last few samples at the end of each symbol, and adding these samples to the start of the symbol. This cyclic prefix (CP) preserves the sub-carrier orthogonality at the expense of wasting some energy, as the power transmitted in the added symbols is not used at the receiver. At the same time, the system data rate is also reduced due to the extension of the total OFDM packet length.

To analyse the effects of a multipath channel on an OFDM signal, a simplified model was developed ignoring GI and background noise. Considering only the direct path signal and one reflected signal with a time delay δ and an attenuation factor of α, the following signal $r(m)$ is detected by the receiver:

$$\begin{aligned} r(m) &= s(m) + \alpha s(m-\delta) \\ &= \sum_{n=0}^{N-1} d_n e^{j\frac{2\pi}{N}nm} + \alpha \sum_{n=0}^{N-1} d_n e^{j\frac{2\pi}{N}n(m-\delta)} \\ &= \sum_{n=0}^{N-1} d_n (1 + \alpha e^{-j\frac{2\pi}{N}n\delta}) e^{j\frac{2\pi}{N}nm}, \qquad m \in [0, N-1]. \end{aligned} \tag{7}$$

Applying demodulation by the FFT, the transmitted data y_n can be recovered from the received signal $r(m)$:

$$\begin{aligned} y_n &= FFT\{r(m)\} \\ &= d_n(1 + \alpha e^{-j\frac{2\pi}{N}n\delta}) \\ &= d_n H(n), \end{aligned} \tag{8}$$

where $H(n) = 1 + \alpha e^{-j\frac{2\pi}{N}n\delta}$ for $n \in [0, N-1]$. As equation (8) indicates, the delayed signal only changes the amplitude $|H(n)|$ and the phase $arg\{H(n)\}$ of each sub-carrier. If the path delay δ is smaller than the length of the GI, no ICI is introduced, and the orthogonality between sub-carriers still holds. Assuming that a 4-QAM modulated signal is being transmitted through this channel, the constellations with different delay spread and attenuation of the detected signal are shown in Fig. 1. As can be seen, the effect of the multipath channel is to expand the constellations on each sub-carrier into different circles surrounding the target points. The number of points on each circle depends on the values of δ and N, and the radius of each circle depends on the value of α. If α is small, the transmitted data can still be correctly decoded. If α is large, and the circles cross over each other, an equaliser is then required to correct the channel distortion. According to equation (8), each received sub-carrier experiences a complex gain $H(n)$ due to the channel. In order to undo this effect, the transmitted data can be recovered from the received signal by multiplying d_n by $1/H(n)$ which is just a single complex multiplication in the frequency domain. It greatly simplifies the equalisation process, especially compared to the adaptive filtering used in single carrier demodulations.

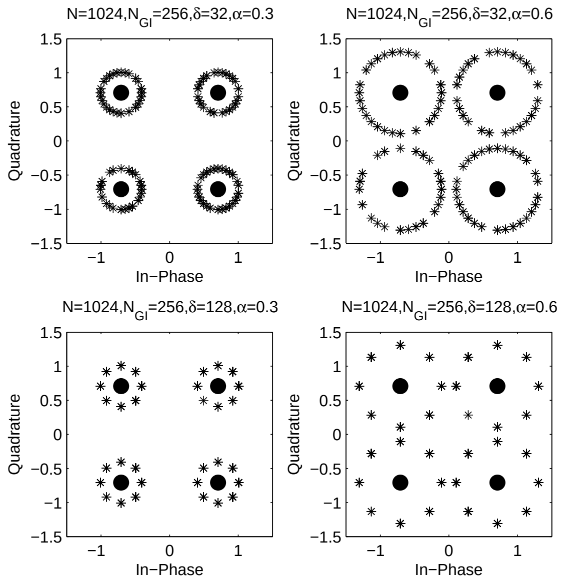

Figure 1: Spread of the 4-QAM OFDM constellations with different delay and amplitude of the reflected signal.

4. Apparatus and experiment set-up

The OFDM method previously described was evaluated using a pair of commercially available SensComp series 600 capacitive ultrasonic transducers [15] for wireless communication. The transducers are composed of a metallised Kapton membrane and a rigid contoured metal backplate with an aperture size of 38.4 mm. They are specially designed for operation in air at an ultrasonic frequency of 50 kHz with a beam angle of 15° at -6 dB. Fig. 2 illustrates the experimental arrangement for ultrasonic wireless communications in air. The data signal was modulated by MATLAB (MathWorks) running on a PC before sending to a TTi TGA 12102 arbitrary waveform generator using GPIB. The signal was then amplified using a Falco WMA-300 high voltage amplifier, and combined with a superimposed +200 V DC bias voltage generated by a Delta Elektronika SM3004-D Power supply. The receiver, identical to the transmitter, was connected to a Cooknell CA6/C charge amplifier powered by a Cooknell SU2/C power supply unit, and followed by a high performance PicoScope 6403A PC oscilloscope. After that, the captured signal was sent back to another PC via a USB interface for signal processing.

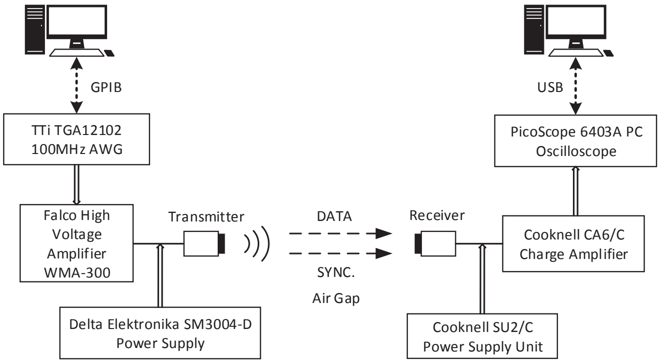

Figure 2: Schematic diagram of the experimental set-up.

The overall system amplitude and phase response through an air gap of 2 m are illustrated in Fig. 3 (a) and (b) respectively. The received impulse was measured by sending a pulse generated by a Panametrics 500PR

Table 1: Parameters of the OFDM signal used in the experiment when transducers are aligned

Parameters	**Settings**
Sampling rate	$f_s = 10$ MHz
Centre frequency	$f_c = 77$ kHz
Signal bandwidth	$B = 45$ kHz
OFDM symbol duration	$T_s = 1$ ms
Sub-carrier spacing	$\Delta f = 1$ kHz
Number of sub-carriers	$N = 45$

pulser from the transmitter to the receiver. As can be seen in Fig. 3 (a), the prominent spectra ranges from 50 kHz up to about 110 kHz. Fig. 3 (b) shows that the phase response of the channel is nearly linear at frequencies between 30 and 170 kHz. The recorded received signal amplitude was typically around 46.6 mV rms at 2 m, and the rms amplitude of the background noise was at about 1.2 mV.

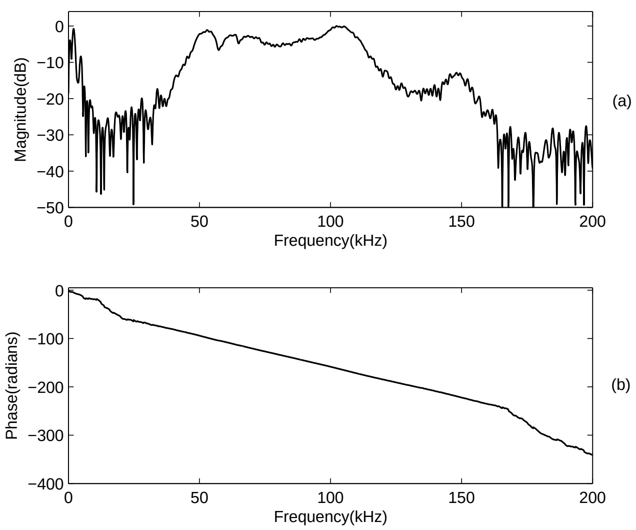

Figure 3: System characteristics: (a) system response and (b) phase response.

All experiments were conducted in an indoor laboratory environment with negligible air turbulence to influence the data transmission. Transmitter and receiver transducers were separated in a LOS manner, and the transmission bandwidth used was from 55 to 99 kHz for best results on a trial and error basis. Parameters of the OFDM signal are listed in Table 1. Sub-carrier signals were modulated using BPSK and two levels of QAM (4-QAM and 16-QAM). The three different modulation schemes from low order to high order were evaluated and compared in the experiments. Note that both 4-QAM and 16-QAM were Gray coded so that for most symbol errors there is only one bit received in error [16].

5. Results and discussion

5.1. Line-of-sight (LOS) transmission

Initial transducer separation was set at 1 m, and different modulated signals with SNRs incremented in 1 dB steps from 5 dB to 18 dB were transmitted. Due to hardware restriction, 90 packets of 45-subchannel OFDM

Table 2: Performances of BPSK, 4-QAM and 16-QAM modulations in an OFDM system

	BPSK	4-QAM	16-QAM
Error-free decoding range (m)	11	9	6
Data rate (kb/s)	45	90	180
Bandwidth efficiency (b/s/Hz)	1	2	4

signal were generated and transmitted continuously through the air channel. The process was repeated 10 times, and then averaged. Therefore, 162000 transmitted bits were observed, allowing the minimal measurable BER of 6.17×10^{-6}. Fig. 4 compares the BER performances of the three modulation schemes in both theory and experiment. As expected, when the noise becomes smaller compared to the signal level, less error occurs. Higher order modulation schemes require a larger SNR to transmit data with fewer bit errors. However, large gaps exist between the theoretical and the experimental BER curves. Note that the theoretical curves are the best achieved BER performance for all three modulation schemes. The discrepancy between theory and experiment results is due to a few reasons. One major reason is the hardware implementation penalty as the received signal was undersampled by 2.34% at the oscilloscope. Therefore, inaccurate timing occurs, and it reduces the orthogonality of the OFDM signal. The second reason is the ISI introduced by multipath interference. Another reason is the bandwidth limitation of the selected ultrasonic transducers. Wider bandwidth transducers may improve the BER performance, especially for high-order modulation schemes. OFDM packet errors for the three modulation schemes were also measured with increased transmission ranges. Error-free decoding was achieved at different ranges for different modulations as listed in Table 2. As the noise margin of BPSK is larger than either 4-QAM or 16-QAM, BPSK holds a more reliable transmission link which is up to 11 m with no measurable bit errors, followed by the error-free decoding ranges for 4-QAM and 16-QAM of 9 m and 6 m, respectively. Table 2 also presents the maximum data transfer rates and the corresponding bandwidth efficiencies for the three modulation schemes. The advantage of using QAM compare to BPSK is that it is able to carry more bits of information per symbol. By increasing the order format of QAM, the data rate of the system as well as the bandwidth efficiency can be significantly increased. It also indicates that each individual sub-carrier can be treated independently from the others in terms of the modulation method used in a self-adaptive system. Thus, a sub-carrier with more channel attenuation can use a more resilient modulation like BPSK or 4-QAM while sub-carriers with better channels can use a higher order modulation like 16-QAM.

To visualise the conditions of the received OFDM signals, constellation diagrams of BPSK, 4-QAM and 16-QAM before and after the phase correction and channel equalisation are given in Fig. 5. As can be seen from Fig. 5 (a) - (c), the raw received signal constellations are corrupted as the constellation points are rotated and spread across the detection boundaries due to phase noise and the effect of the ultrasonic channel. After phase noise correction and channel equalisation, as shown in Fig. 5 (d) - (f), both the phase rotation and amplitude distortion have been corrected with the aid of a known pilot signal. Note this pilot signal contains randomly generated bits modulated in the same way as the OFDM signal, and was transmitted along with the information signal.

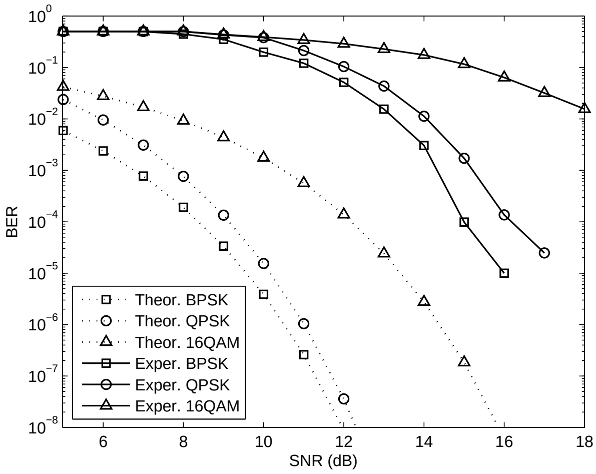

Figure 4: Theoretical and experimental bit error rate performance of three different OFDM modulation schemes at 1 m range.

5.2. Reflected and diffracted signals

The maximum beam divergence angle of the ultrasonic signal at 55 kHz used in the experiment was 11.4°. Thus, the emitted ultrasonic signals were relatively directional. Similarly, the receiver can only detect signals with small incidence angles. In this case, when the transducers are aligned in a LOS manner, most undesired reflections can be eliminated. In the situations when the transducer centre normals are not coincident and the receiver transducer is close to possible reflectors such as the floor and walls, reflected signals can then be detected. Diffraction also occurs in practice. This can be seen as the deflection or 'bending' of the waves, caused by an obstacle in the propagation path or by nonhomogeneity of the air [17]. The effects of diffraction can be evaluated by measuring signal levels for different frequencies diffracted from a sharp-edged screen. Fig. 6 shows the configuration of transmitter transducer (Tx), receiver transducer (Rx), and a blocking screen, where the lateral displacement u of the receiver can vary with the transmitter and receiver transducer faces in parallel (position A). It should be noted that the screen occluded half of the transmitted aperture when $u = 0$, and only diffracted signals could be obtained when $u \geq 0.0192$ m and no LOS signal could be received. Fig. 7 shows the resulting signal attenuation at the receiver Rx as a function of u, for the highest signal frequency (99 kHz) and the lowest signal frequency (55 kHz) used in the experiment. It can be seen that for both low and high frequency signals, the larger the lateral displacement, the smaller amount of diffracted energy that is received, as expected. In addition, the low frequency signals are diffracted more than the high frequency signals and can be detected at larger values of lateral displacement. However, when the lateral displacement is as small as 0.2 m for example, the signal attenuation for high and low frequency waves was approximately -30 dB and -19 dB respectively.

The reduction of sound pressure level due to diffraction around the edge of a barrier can be described in terms of a Fresnel number [17, 18], which is given by

$$N = \frac{2}{\lambda}(d_1 + d_2 - d) \tag{9}$$

where λ is the wavelength of sound and lengths d_1, d_2, and d are as shown in Fig. 6. The attenuation by diffraction A_d, in dB, is then approximated as a function of the Fresnel number

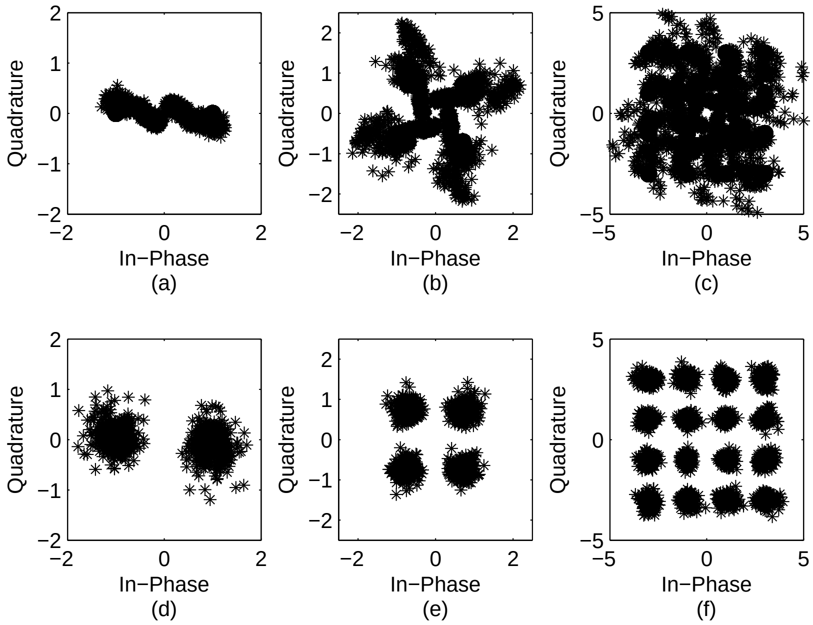

Figure 5: Received constellations before (a) - (c) and after (d) - (f) phase noise correction and channel equalisation for BPSK-OFDM, 4QAM-OFDM and 16QAM-OFDM at 11 m, 9 m and 6 m respectively.

$$A_d = 10log_{10}(20N). \tag{10}$$

These diffraction effects were incorporated into an earlier model of the ultrasonic channel [19] that accurately predicted the LOS channel response in air, accounting for beam spread and attenuation along the propagation path. Equation (10) yields the two attenuation curves for 55 kHz and 99 kHz signals in Fig. 7. As can be seen, the theoretical prediction matches the experimental data well. Note that the model only considers a point source and receiver, therefore the actual received signal energy may decrease faster than the theoretical prediction with the increase of lateral displacement as the effective reception area of the receiver is an ellipse rather than a circle. By using the same diffraction setup in Fig. 6, the BER results for all three modulation schemes with increasing lateral displacements up to 0.2 m are shown in Fig. 8. As can be seen, the BER curves for all three modulations ascend rapidly with lateral displacement. 16-QAM, with the most spreading of the spots in the constellation and hence with reduced noise immunity, experienced the most error decoding at all ranges. Lower-order modulation schemes, 4-QAM and BPSK, proved their superiority over 16-QAM when signals are diffracted around a sharp-edged screen, with first bit errors occurring at 0.1 m and 0.125 m, respectively. When the lateral displacement of the receiver increased to 0.2 m, the BERs for all three modulations reached a level close to 30%. It indicates that BPSK and 4-QAM modulation schemes work better using only diffracted signals than 16-QAM in terms of BER performance. However, non-LOS transmission with no measurable errors was achieved with BPSK-OFDM and 4QAM-OFDM.

One situation that occurs when the face of the receiver is angled towards the edge of the screen barrier is illustrated in Fig. 6 position B. The theoretical signal attenuation for 55 kHz and 99 kHz signals with an increasing oblique angle θ from 0° to 40° in a 5° step are compared with experimental results in Fig. 9, and good agreement was found between the two. Accordingly, the BER results for the three modulation schemes are illustrated in Fig. 10. It shows a similar overall trend as the curves in Fig. 8. For 4-QAM and BPSK, the two modulation methods experienced signal error-free decoding with oblique angles up to 10° and 20°, respectively.

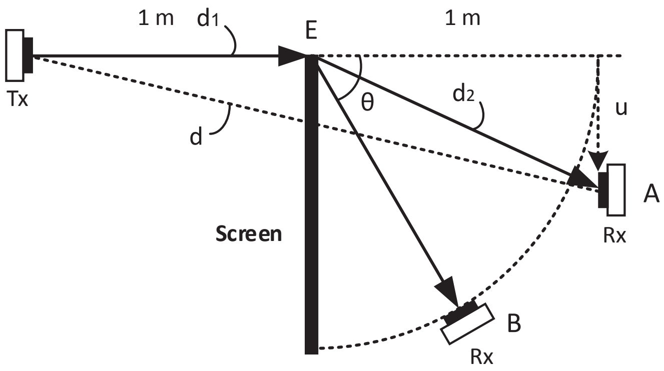

Figure 6: Configuration of transmitter Tx and receiver Rx where ultrasonic waves diffract around the edge of a blocking screen. Position A: transducer faces parallel, position B: receiver rotates and faces the edge E.

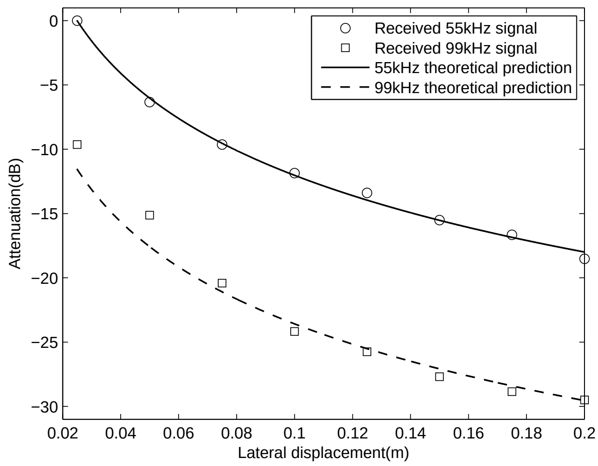

Figure 7: Theoretical and experimental signal attenuation for 55 kHz and 99 kHz ultrasonic waves with varied lateral displacement in a diffraction setup consisting of a sharp-edged screen.

5.3. Transmission in a multipath environment

In practice, the effect of multipath reflections cannot be ignored. It can lead to the superposition of several time-delayed and attenuated copies of the transmitted signal at the receiver. As a result, it may introduce spreading of the received signal in time and constructive and destructive interference at various frequencies, leading to frequency selectivity. A typical reflection pattern in the time domain is shown in Fig. 11 when a Hamming-windowed 10-cycle 55 kHz sinusoid signal was transmitted through the system in the presence of a reflecting surface. The enlarged region in Fig. 11 shows two strong reflections followed by additional signals with much smaller amplitudes within 2 ms of the direct signal. Each pattern of peaks corresponded to the arrival of acoustic reflections at the receiver at different moments in time. It should be noted that all the reflections are relatively weak compared with the direct signal due to the directivity of the receiver. To combat both ISI and ICI, a CP with a length of 2 ms was then added to the OFDM symbols. Accordingly, the length of the OFDM symbols should also be extended. Details of the parameter settings are listed in Table 3. Since the OFDM symbol length was extended to 8 ms, to preserve sub-carrier orthogonality, the sub-channel width was reduced

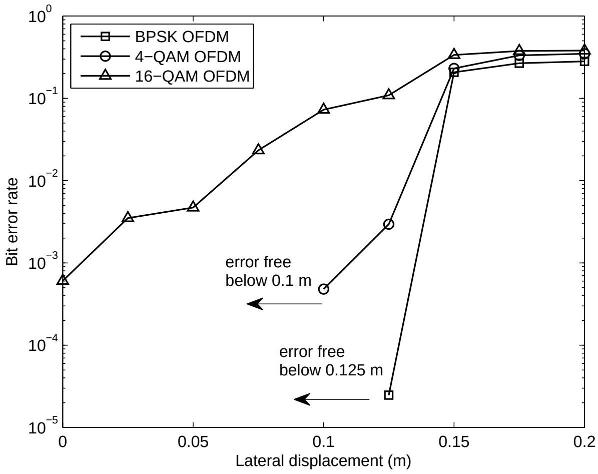

Figure 8: BERs with varied lateral displacement in a diffraction setup consisting of a sharp-edged screen using BPSK, 4-QAM and 16-QAM modulations, showing error-free non-LOS transmission ranges for BPSK-OFDM and 4QAM-OFDM.

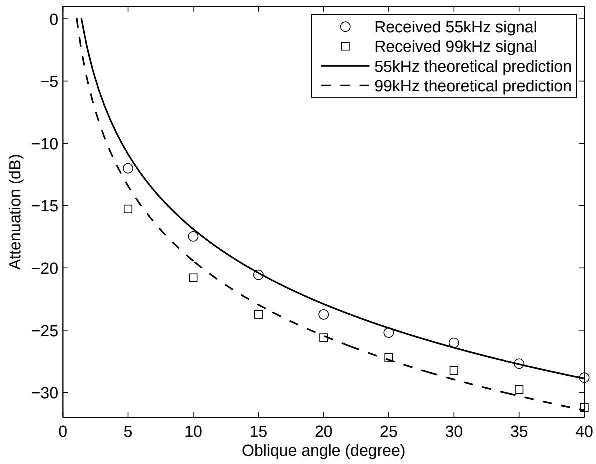

Figure 9: Theoretical and experimental signal attenuation for 55 kHz and 99 kHz ultrasonic waves with varied oblique angles in a diffraction setup consisting of a sharp-edged screen.

to only 125 Hz with a total number of 360 sub-carriers in the range of 55 to 99 kHz. The tested error-free decoding ranges for BPSK, 4-QAM and 16-QAM were maintained the same as listed in Table 2 using this new channel arrangement. However, after adding the CP, total data transfer rates for all three modulation schemes were reduced by 20%. To evaluate the performance of using CP in a multipath environment, BERs of the OFDM signals with CP and without CP are compared in Fig. 12. It is observed that there is an improvement in BER after adding CP, especially when the received signal has a large SNR. Note that only the performance of 16-QAM OFDM signals are presented here as an illustrative example. Accordingly, the constellations of the equalised 16-QAM signals without and with CP at a SNR value of 32 dB are shown in Fig. 13 (a) and (b), respectively. As can be seen, more concentrated constellation points with less spreading were extracted from the OFDM signal after adding CP.

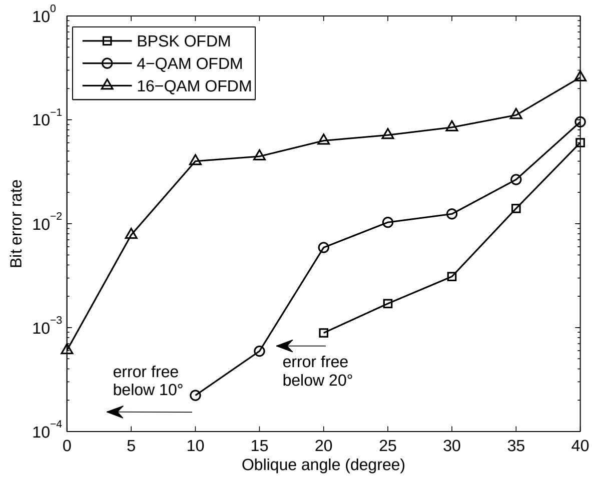

Figure 10: BERs with varied oblique angles when the receiver is facing towards the edge of the blocking screen using BPSK, 4-QAM and 16-QAM modulations.

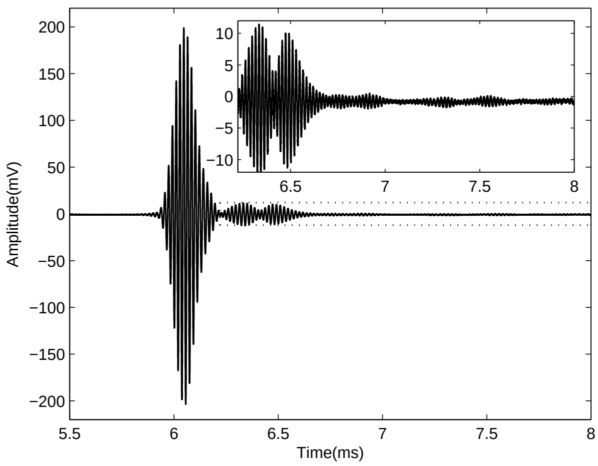

Figure 11: Received direct signal and reflected signals in a multipath environment.

6. Conclusions

This paper evaluated an airborne multiple-channel OFDM data communication system using a pair of commercially available capacitive ultrasonic transducers. The main advantage of the multiple-channel OFDM modulation scheme was that it enabled channel equalization in the frequency domain, thus eliminating the need for potentially complex time-domain equalizers. It also provided a data transmission robust against both ICI and ISI caused by the multipath channel. Due to hardware limitations, most air-coupled capacitive ultrasonic transducers have a relatively narrow bandwidth to provide data communication with an acceptable transfer rate. OFDM modulation can maximise bandwidth utility by allowing sub-carriers to overlap each other. Different order baseband modulation schemes from BPSK, 4-QAM and 16-QAM were implemented in the OFDM system using an ultrasonic band from 55 to 99 kHz and individual performances were evaluated. The maximum data rate achieved in this work was 180 kb/s using 16-QAM OFDM in a LOS manner. BPSK-OFDM experienced the lowest decoding errors when using the same signal power, thus the longest error-free decoding range achieved was up to 11 m with a data rate of 45 kb/s. It was shown by experiment that all three modulation schemes investigated could operate in a non-LOS configuration after diffracting around a sharp-edged screen, and that

Table 3: Parameters of the OFDM signal used in the experiment in a multipath environment

Parameters	**Settings**
Sampling rate	$f_s = 10$ MHz
Centre frequency	$f_c = 77$ kHz
Signal bandwidth	$B = 45$ kHz
OFDM symbol duration	$T_s = 8$ ms
Cyclic prefix length	$T_{cp} = 2$ ms
Sub-carrier spacing	$\Delta f = 125$ Hz
Number of sub-carriers	$N = 360$

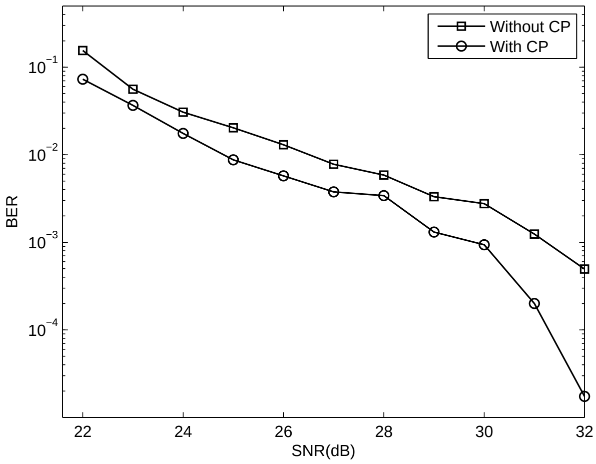

Figure 12: Bit error rate performance for 16-QAM OFDM modulation with and without cyclic prefix..

BPSK-OFDM was proven to return the best BER performance when only diffracted signals are received in the channel. In a dispersive environment with multipath interference, system BER can be significantly reduced by adding CP to the OFDM symbols, however, at the expense of losing 20% of the transmitted signal and overall data transfer rate. Future work will focus on establishing a full-duplex air-coupled ultrasonic data communication network for indoor applications by implementing OFDM modulation.

Acknowledgements

This work was supported by Science Foundation Ireland (SFI) Research Frontiers Programme grant number 11/RFP.1/ECE/3119.

References

[1] R. Adler, P. Desmares, J. Spracklen, An ultrasonic remote control for home receivers, Consumer Electronics, IEEE Transactions on CE-28 (1) (1982) 123–128.

[2] S. Holm, O. Hovind, S. Rostad, R. Holm, Indoors data communications using airborne ultrasound, in: Acoustics, Speech, and Signal Processing, 2005. Proceedings. (ICASSP '05). IEEE International Conference on, Vol. 3, 2005, pp. 957–960.

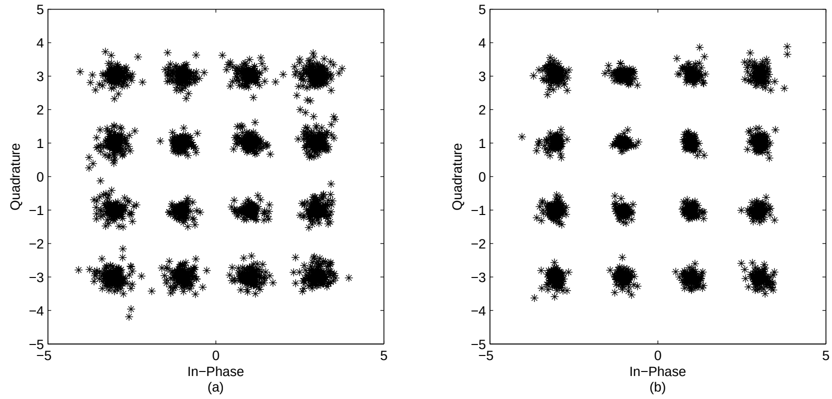

Figure 13: Received 16-QAM OFDM signal constellations after equalisation (a) without CP and (b) with CP at a SNR value of 32 dB.

[3] M. Hazas, A. Hopper, Broadband ultrasonic location systems for improved indoor positioning, Mobile Computing, IEEE Transactions on 5 (5) (2006) 536–547.

[4] C. Li, D. Hutchins, R. Green, Short-range ultrasonic digital communications in air, Ultrasonics, Ferroelectrics and Frequency Control, IEEE Transactions on 55 (4) (2008) 908–918.

[5] C. Li, D. Hutchins, R. Green, Short-range ultrasonic communications in air using quadrature modulation, Ultrasonics, Ferroelectrics and Frequency Control, IEEE Transactions on 56 (10) (2009) 2060–2072.

[6] K. Nakamura (Ed.), Ultrasonic Transducers: Materials and Design for Sensors, Actuators and Medical Applications, Woodhead Publishing Limited, 2012.

[7] S. Weinstein, The history of orthogonal frequency-division multiplexing [history of communications], Communications Magazine, IEEE 47 (11) (2009) 26–35.

[8] W. M. D. Wright, O. Doyle, C. T. Foley, Multi-channel data transfer using air-coupled capacitive ultrasonic transducers, in: Ultrasonics Symposium, 2006. IEEE, 2006, pp. 1805–1808.

[9] A. Ens, L. Reindl, Multicarrier airborne ultrasound transmission with piezoelectric transducers, Ultrasonics, Ferroelectrics, and Frequency Control, IEEE Transactions on 62 (5) (2015) 905–914.

[10] J. Proakis, M. Salehi, Digital Communications, McGraw-Hill Higher Education, 2008.

[11] S. Weinstein, P. Ebert, Data transmission by frequency-division multiplexing using the discrete fourier transform, Communication Technology, IEEE Transactions on 19 (5) (1971) 628–634.

[12] M. Skolnik, Introduction to Radar Systems, Electrical engineering series, McGraw Hill, 2001.

[13] P. Lazik, A. Rowe, Indoor pseudo-ranging of mobile devices using ultrasonic chirps, in: Proceedings of the 10th ACM Conference on Embedded Network Sensor Systems, SenSys '12, ACM, New York, NY, USA, 2012, pp. 99–112.

[14] D.-C. Chang, Effect and compensation of symbol timing offset in ofdm systems with channel interpolation, Broadcasting, IEEE Transactions on 54 (4) (2008) 761–770.

[15] Senscomp, inc. the senscomp website. (Jan. 2016).
URL `http://www.senscomp.com/pdfs/series-600-environmental-grade-sensor.pdf`

[16] E. McCune, Practical digital wireless signals, Cambridge University Press, 2010.

[17] M. J. Crocker, Handbook of Acoustics, A Wiley-Interscience Publication, Wiley, 1998.

[18] N. H. F. Thomas D. Rossing, Principles of Vibration and Sound, Springer, 2004.

[19] W. Jiang, W. M. D. Wright, Multichannel ultrasonic data communications in air using range-dependent modulation schemes, Ultrasonics, Ferroelectrics, and Frequency Control, IEEE Transactions on 63 (1) (2016) 147–155.